



HAL
open science

Toxoplasma gondii chronic infection decreases visceral nociception through peripheral opioid receptor signaling

Alexis Audibert, Xavier Mas-Orea, Lea Rey, Marcy Belloy, Emilie Bassot, Gilles Marodon, Frédérick Masson, Nicolas Cenac, Gilles Dietrich, Chrystelle Bonnart, et al.

► To cite this version:

Alexis Audibert, Xavier Mas-Orea, Lea Rey, Marcy Belloy, Emilie Bassot, et al.. Toxoplasma gondii chronic infection decreases visceral nociception through peripheral opioid receptor signaling. 2024. hal-04740282

HAL Id: hal-04740282

<https://hal.science/hal-04740282v1>

Preprint submitted on 28 Oct 2024

HAL is a multi-disciplinary open access archive for the deposit and dissemination of scientific research documents, whether they are published or not. The documents may come from teaching and research institutions in France or abroad, or from public or private research centers.

L'archive ouverte pluridisciplinaire **HAL**, est destinée au dépôt et à la diffusion de documents scientifiques de niveau recherche, publiés ou non, émanant des établissements d'enseignement et de recherche français ou étrangers, des laboratoires publics ou privés.

1 ***Toxoplasma gondii* chronic infection decreases visceral nociception through**
2 **peripheral opioid receptor signaling**

3
4 Alexis Audibert 1,2, Xavier Mas-Orea 2, Léa Rey 2, Marcy Belloy 1, Emilie Bassot 1, Gilles Marodon 3, Frederick
5 Masson 1, Nicolas Cenac 2, Gilles Dietrich 2, Chrystelle Bonnart 2*[@](mailto:nicolas.blanchard@inserm.fr), Nicolas Blanchard 1*[@](mailto:chrystelle.bonnart@inserm.fr)

6
7 1 Toulouse Institute for Infectious and Inflammatory Diseases, Infinity, Inserm, CNRS, University Toulouse III,
8 Toulouse, France

9 2 IRSD, Inserm, INRAE, ENVT, University Toulouse III - Paul Sabatier (UPS), Toulouse, France

10 3 Centre d'Immunologie et des Maladies Infectieuses (CIMI-PARIS), Inserm, CNRS, Sorbonne University, Paris,
11 France

12
13 * co-senior authors

14 @ co-corresponding authors

15 Nicolas Blanchard (nicolas.blanchard@inserm.fr)

16 Chrystelle Bonnart (chrystelle.bonnart@inserm.fr)

19 **Abstract (149 words)**

20 By eliciting immune activation in the digestive tract, intestinal pathogens may perturb gut homeostasis. Some
21 gastrointestinal infections can indeed increase the risk of developing post-infectious irritable bowel syndrome
22 (PI-IBS). Intriguingly, the prevalent foodborne parasite *Toxoplasma gondii* has not been linked to the
23 development of PI-IBS and the impact of this infection on colon homeostasis remains ill-defined. We show in a
24 mouse model that latent *T. gondii* decreases visceral nociceptive responses in an opioid signaling-dependent
25 manner. Despite the accumulation of Th1 and cytotoxic T cells in the colon of latently infected mice, the
26 selective invalidation of enkephalin gene in T cells ruled out the involvement of T cell-derived enkephalins in
27 hypoalgesia. These findings provide clues about how this widespread infection durably shapes the gut immune
28 landscape and modifies intestinal physiological parameters. They suggest that in contrast to other gut
29 microbes, *T. gondii* infection could be negatively associated with abdominal pain.

30

31

32 Introduction

33 Most often, infections are rapidly resolved, allowing the organism to return to its initial state. However, in some
34 cases, infections can have long-lasting consequences, thereby negatively or positively regulating the
35 development of chronic diseases ¹⁻³. As examples, a mouse model suggested that early-life brain viral infection
36 can predispose to the development of brain autoimmune disease during adulthood ⁴ and in humans, Epstein-
37 Barr virus infection increases by over 30-fold the risk to develop multiple sclerosis ⁵.

38 As one of the largest interface between the host and the environment, the gastrointestinal (GI) tract is highly
39 exposed to pathogens, which can profoundly shape the mucosal immune environment ⁶. The GI tract is
40 composed of different cellular layers. Below the epithelium which surface is exposed to the gut microbiota, lie
41 (i) a lamina propria containing fibroblasts and immune cells, (ii) muscular layers, and (iii) a neuronal network
42 divided into an intrinsic (enteric nervous system, ENS) and extrinsic peripheral neuronal compartment. These
43 entities exert specific functions that are crucial for tissue homeostasis. The ENS regulates intestinal functions
44 such as gut motility, secretion, permeability, and blood flow. Extrinsic neurons relay peripheral information,
45 such as visceral pain, to the central nervous system (CNS) through afferent projections from neurons
46 (nociceptors) that have their soma in the dorsal root ganglia (DRG). Visceral pain transmitted by nociceptors
47 results from the integration of excitatory (pro-nociceptive) and inhibitory (anti-nociceptive) signals present
48 within the surrounding environment. Pro-nociceptive mediators like pro-inflammatory cytokines or some
49 proteases ⁷, increase nociceptor firing, leading to visceral hypersensitivity, while anti-nociceptive mediators
50 such as endogenous opioids, decrease nociceptor activity, thus relieving visceral pain ⁸⁻¹⁰. As drivers of
51 inflammatory mediators, several intestinal pathogens causing infectious gastroenteritis enhance pro-
52 nociceptive signals and increase the risk of developing Irritable Bowel Syndrome (IBS), a phenomenon known
53 as Post-Infectious IBS (PI-IBS) ¹¹. According to Rome IV criteria, IBS is a functional chronic disorder characterized
54 by changes in bowel habits and abdominal pain without obvious gut inflammation or macroscopic lesions ¹². In
55 humans, PI-IBS has been reported following infections with pathogens such as bacteria (*Escherichia coli*,
56 *Salmonella*, *Campylobacter jejuni*), parasites (*Giardia intestinalis* ¹³, *Cryptosporidium* ¹⁴) and viruses (*Norovirus*
57 ¹⁵), suggesting that common immune-mediated mechanisms possibly trigger the development of this syndrome
58 ¹⁶. Interestingly, one study suggested that visceral hypersensitivity in PI-IBS could arise from prolonged
59 nociceptor activation and sensitization due to incomplete resolution of immune responses, thus leading to
60 persistent abdominal pain despite apparent recovery from acute gastroenteritis ¹⁷. Moreover, *Blastocystis*-
61 infected rats exhibit a PI-IBS-like phenotype characterized by a non-inflammatory visceral hypersensitivity ¹⁸
62 and *Citrobacter rodentium* infection of mice evokes hyperexcitability of colonic DRG neurons which persists
63 following resolution of the infection ¹⁹, indicating that IBS features can be recapitulated in animal models of
64 infection. Intriguingly, there is currently no epidemiological evidence that the highly prevalent foodborne
65 parasite *Toxoplasma gondii* (*T. gondii*) is linked to the development of PI-IBS.

66 *T. gondii* is an obligate intracellular protozoan parasite able to infect any warm-blooded animal, including
67 humans. It is estimated that around 30% of the world population, reaching up to 50% in some areas, has been
68 exposed to this parasite ²⁰. Infection occurs after ingestion of contaminated food or water, allowing parasite
69 cysts or oocysts to penetrate the gut and invade the host through the small intestine. Parasites then proliferate
70 as fast-replicating tachyzoites, causing tissue inflammation, bacterial translocation, and strong type 1 immune
71 responses including durable Th1 CD4+ T cell responses ^{6,21,22}. During this initial acute phase of infection,
72 tachyzoites disseminate systemically and reach the CNS, where chronic infection is established. The long-term
73 chronic phase is characterized by clearance of the parasite from the periphery (including the gut) and
74 persistence of the parasite in the CNS, retina and skeletal muscles in the form of slow-replicating bradyzoites
75 located within intracellular cysts ^{23,24}. While the impact of *T. gondii* chronic infection on brain function has been
76 extensively studied ^{25,26}, much less is known about the potential long-term consequences of *T. gondii* infection
77 on gut homeostasis. One pioneer study has reported that by inducing bacterial translocation during the acute
78 phase, *T. gondii* infection promotes the development of microbiota-specific CD4+ memory T cells with a pro-
79 inflammatory Th1 phenotype. Interestingly, these T cells can persist in the gut for more than 200 days post-
80 infection ²². More recently, it was shown that chronic *T. gondii* infection exacerbates the severity of intestinal
81 damage caused by chemical injury, due to heightened activation status of monocytes in chronically infected
82 mice ²⁷. In rats, chronic *T. gondii* infection has been reported to cause damage of the colonic mucosa and induce
83 death of some neurons of the submucosal or myenteric ENS plexi, without altering the gastrointestinal transit
84 time or the fecal pellet output ^{28,29}.

85 Together, these data suggest that as other intestinal pathogens, by shaping the neuroimmune environment of
86 the gut, *T. gondii* infection could promote the development of PI-IBS. To address this question, we explored
87 the long-term consequences of latent *T. gondii* infection on the colonic microenvironment and on visceral
88 nociceptive responses. Contrary to our expectations, we found that chronic *T. gondii* infection decreases
89 visceral nociception in an opioid receptor signaling-dependent manner, in the absence of macroscopic colonic
90 inflammation. This effect was associated with a long-lasting increase in colonic T cells displaying a Th1 or
91 cytotoxic phenotype, but could not be explained by T cell-produced enkephalins. These findings shed light on
92 the long-term impact of this widespread foodborne infection on the gut neuroimmune landscape and
93 physiology.

94

95

96 **Results**

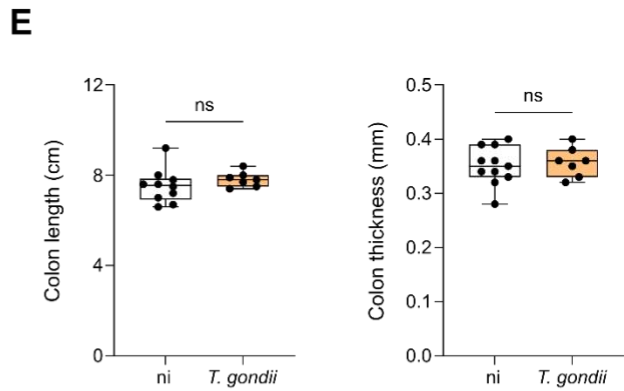
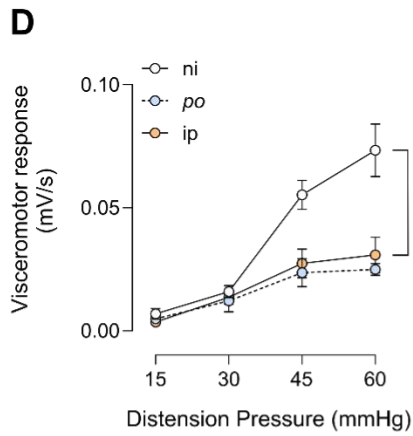
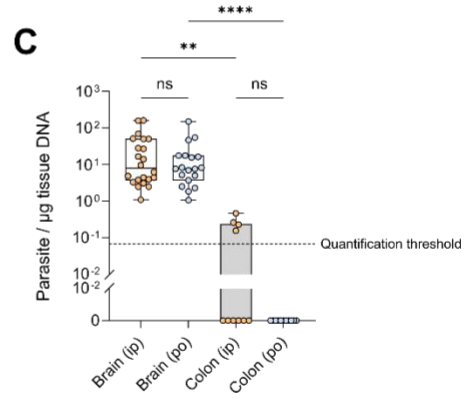
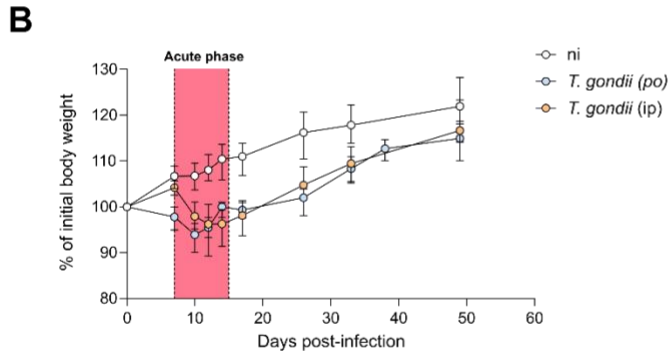
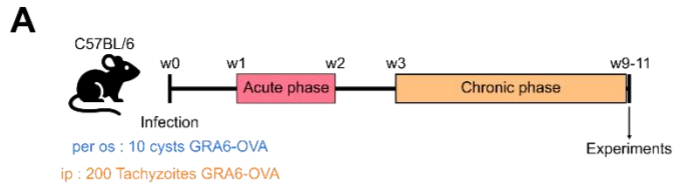
97 ***Toxoplasma gondii* chronic latent infection decreases visceral nociceptive responses**

98 As C57BL/6 mice are naturally susceptible to *T. gondii* infection and develop encephalitis following
99 infection with a type II strain, we used an established model of infection of C57BL/6 mice with a modified type
100 II strain expressing the immunodominant GRA6-OVA model antigen (Pru.GFP.GRA6-OVA), which elicits a strong
101 CD8+ T cell response able to effectively control the parasite burden during chronic stage³⁰, thereby mimicking
102 the pathophysiology of latent human infection. To examine the importance of the primary intestinal phase of
103 infection on the pathophysiological outcome, mice were infected either *per os* by administration of 10 cysts or
104 intraperitoneally (ip) by injection of 200 tachyzoites (**Fig. 1A**). As previously reported³¹, *T. gondii* infection
105 induced a transient weight loss during the acute phase of infection (**Fig. 1B**), whatever the mode of parasite
106 administration. At 10 weeks post-infection (pi), none of the *per os*-infected mice exhibited detectable parasite
107 burden in the colon while some ip-infected mice still had detectable parasites in the colon. Both models
108 displayed similar parasite loads in the brain (**Fig. 1C**).

109 To assess visceral sensitivity in non-infected (ni) *versus* chronically infected mice (*per os* or ip, 10 weeks post-
110 infection), we measured the visceromotor response (VMR) elicited by colorectal distension. In this assay, VMR
111 measurements are directly linked to the stimulus intensity evoked by increasing pressures of a balloon inserted
112 into the distal colon. Strikingly, compared to uninfected mice, both *per os* and ip-infected mice exhibited a
113 significant reduction of VMR in response to colorectal distension (**Fig. 1D**). Hence, *T. gondii* chronic infection
114 decreases visceral nociceptive responses regardless of the mode of infection, and thus regardless of local
115 parasite persistence (as parasite load was undetectable in the colon of *per os* chronically infected mice, see **Fig.**
116 **1C**). Since visceral hypoalgesia was similarly induced following *per os* and ip routes of infection, and since ip
117 infections avoid the use of 'reservoir' mice required to prepare the cysts, we conducted the rest of the study
118 with ip-infected mice.

119 To start deciphering the mechanisms explaining this hypoalgesia, we assessed the presence of potential
120 anomalies of the colonic tissue at macroscopic and microscopic levels. Colon thickness and length were not
121 changed at 10 weeks post-infection, showing that this model of chronic latent infection does not induce a
122 macroscopic long-lasting colonic inflammation (**Fig. 1E**). Moreover, H&E stainings of the colon showed that
123 chronically infected mice have a normal architecture and do not display any microscopic damage or massive
124 immune infiltration (**Fig. 1F**). Together, these data indicate that latent *T. gondii* infection decreases visceral
125 nociception independently from the route of infection, and in the absence of apparent gut inflammation.

126



128 **Figure 1: *Toxoplasma gondii* chronic infection decreases visceral nociceptive responses in the absence of**
129 **macroscopic colonic inflammation**

130 **(A)** Experimental workflow: C57BL/6 mice were infected with Pru.GFP.GRA6-OVA *T. gondii* either *per os* with 10 cysts or by
131 intraperitoneal injection with 200 tachyzoites. Experiments were performed between 9 and 11 weeks post-infection. **(B)** Weight
132 measurements during the course of infection, relative to the initial body weight. Dots represent the median +/- IQR of n = 37 (ni), 22
133 (ip), or 29 (*per os*) mice. **(C)** Parasite burden per μg of tissue DNA measured by qPCR on genomic DNA extracted from brain and colon.
134 Box and whisker plots show median +/- IQR. Data are from 3 pooled independent experiments with each dot representing one mouse.
135 Statistical analysis was performed with Kruskal-Wallis test and subsequent Dunn's correction for multiple comparisons. **(D)**
136 Visceromotor response (VMR) to increasing colorectal distension pressure (15 to 60 mm Hg) measured in non-infected (ni) mice or mice
137 infected either *per os* or ip. Data are shown as mean +/- SEM and correspond to 3 pooled experiments with n = 15 (ni), 6 (*per os*), and
138 12 (ip) mice. Statistical analysis was performed with Areas Under the Curve (AUC) using a Kruskal-Wallis test with Dunn's correction for
139 multiple comparisons. **(E)** Colon length was measured and colon was opened longitudinally to measure thickness. Data are from 1
140 experiment, representative of 2 independent experiments. Statistical analysis was performed using Mann-Whitney test. **(F)**
141 Representative image of Hematoxylin/Eosin staining of distal colon section (5 μm thick) from ni vs. ip-infected mice. Scale bar = 200 μm .

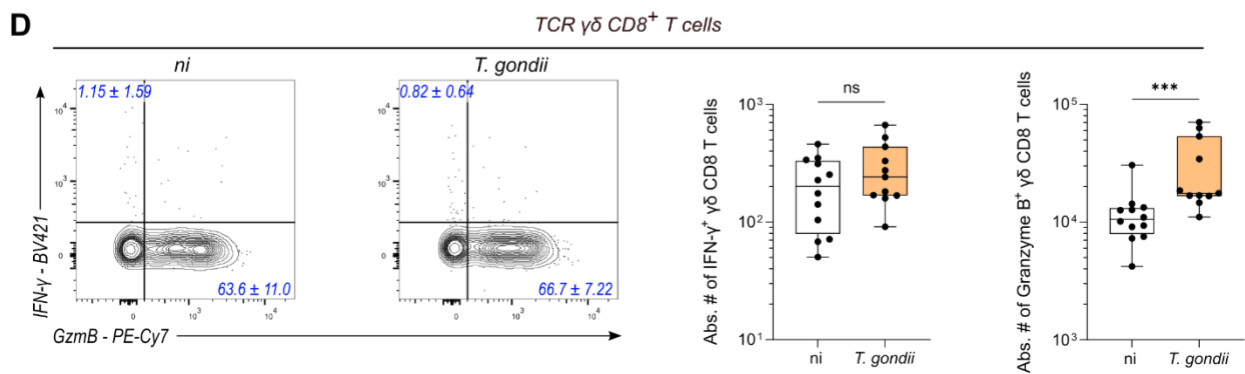
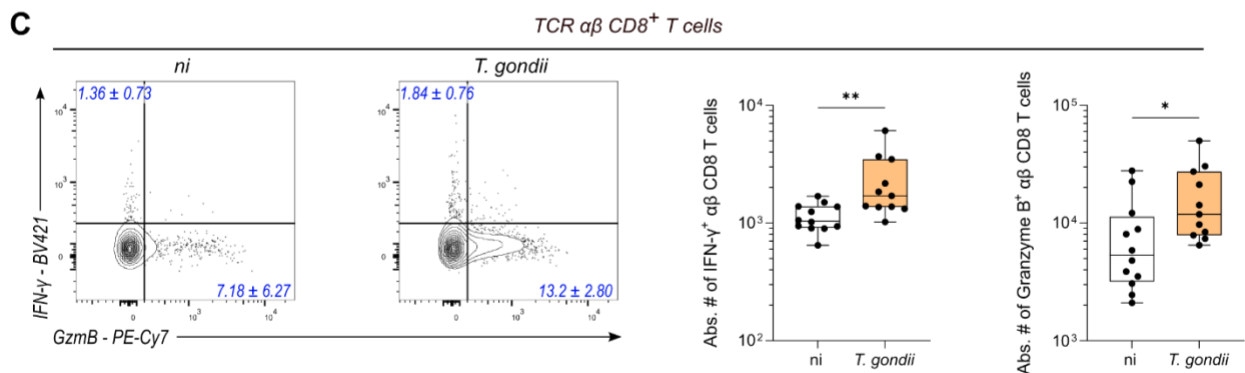
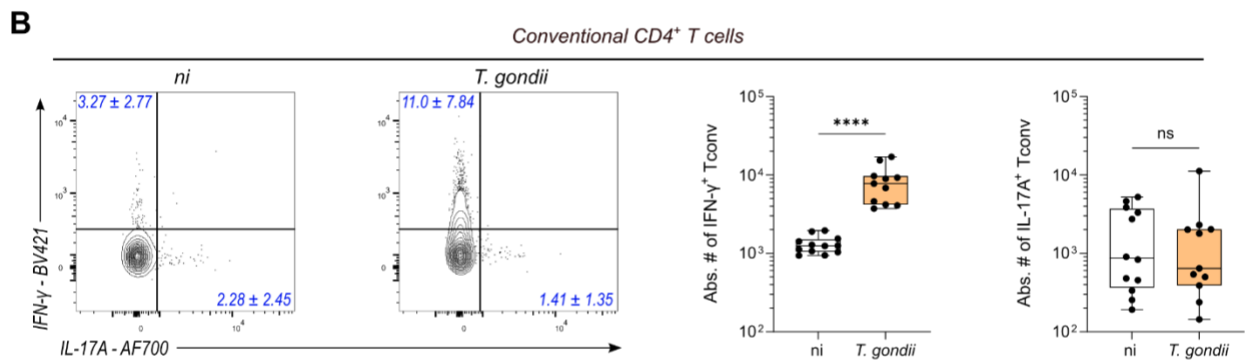
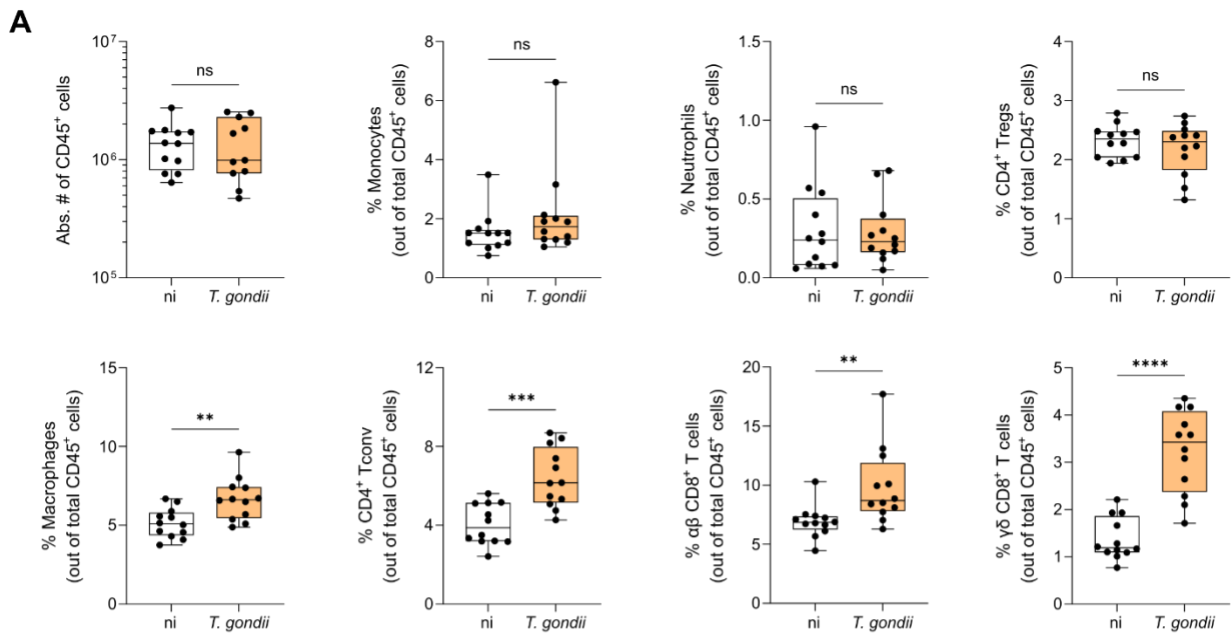
142

143 ***Toxoplasma gondii* chronic infection induces long-lasting modifications of the colonic immune landscape**

144 In line with the fact that *T. gondii* infection has not been reported to be a trigger of PI-IBS, mice chronically
145 infected with *T. gondii* exhibited lower visceral response to colorectal distension. This result suggests that
146 analgesic pathways are mobilized in *T. gondii* infected mice, possibly explaining the diminished VMR observed
147 upon chronic infection. Several studies have highlighted the role of immune cells and mediators in modulating
148 visceral sensitivity and pain³²⁻³⁵. Therefore, we investigated potential changes in colonic immune infiltration
149 during *T. gondii* infection.

150 First, we set out to analyze the main immune cell modifications occurring in the colon shortly after infection
151 (i.e. at acute stage). To this aim, we performed an unsupervised flow cytometry analysis of colonic cells
152 extracted from the colon of non-infected mice vs mice infected with *T. gondii* for 14 days. This analysis indicated
153 that the colon of acutely infected mice is enriched in both innate and adaptive immune cells (**Fig. S1**). More
154 specifically, the colon of acutely infected mice exhibited a higher proportion of monocytes (cluster 3) and
155 neutrophils (cluster 1) compared to non-infected mice (**Fig. S1A-B**). In addition, various T cell subsets were
156 enriched (**Fig. S1C-D**), such as IFN- γ -producing CD4+ T cells (clusters 4 & 15), cytotoxic CD8+ T cells (clusters 7
157 & 2) and T cells producing both IFN- γ and Granzyme B (clusters 5, 6 & 8). In contrast, we found a lower
158 percentage of regulatory (FoxP3+) CD4+ T cells (cluster 3) and of IL-17-producing conventional (FoxP3-) CD4+ T
159 cells (cluster 9) in acutely infected compared to non-infected mice. These data confirmed that acute infection
160 by *T. gondii* is associated with a type 1-polarized immune response, and they allowed us to identify the immune
161 cell subsets of the colon which proportions are most affected (negatively or positively) following *T. gondii*
162 infection.

163 We next conducted supervised flow cytometry analyses to investigate how the abundance of such immune cell
164 subsets changed throughout chronic infection. The gating strategies used to identify the different immune cell
165 subsets are depicted in **Fig. S2**. First, in contrast to acute infection, we observed no change in the number of
166 leukocytes (i.e. CD45+ Epcam-negative) present in the colon of chronically infected mice compared to non-
167 infected mice, indicating that immune infiltration of the colon has fully resolved at chronic stage (**Fig. 2A**), in
168 agreement with the normal histology described above (see **Fig. 1E-F**). This observation was corroborated by
169 the similar percentages of monocytes, neutrophils and Tregs in the colon of non-infected vs. chronically infected
170 mice (**Fig. 2A**). Yet, the composition of the colonic immune compartment remained durably changed upon
171 infection since infected mice showed a significant increase in the proportion of macrophages (F4/80+, CD11b+,
172 Ly6C/G-), conventional CD4+ T cells (Foxp3-) and both TCR $\alpha\beta$ + CD8+ and TCR $\gamma\delta$ + CD8+ T cells (**Fig. 2A**). In
173 addition, T cells from infected mice were more prone to produce effector molecules after PMA/ionomycin
174 restimulation, as demonstrated by the higher number of IFN- γ -positive conventional CD4+ T cells and TCR $\alpha\beta$
175 CD8+ T cells and the higher number of granzyme B-positive (reflecting cytotoxicity) TCR $\alpha\beta$ + CD8+ and TCR $\gamma\delta$ +
176 CD8+ T cells in the colon of *T. gondii*-infected mice (**Fig. 2B-D**). In conclusion, while the proportions of
177 neutrophils, monocytes and Tregs out of CD45+ leukocytes normalized over time, chronic infection by *T. gondii*
178 induced long lasting modifications of the colonic immune landscape, characterized by an enrichment in
179 macrophages, cytotoxic CD8+ T cells and IFN- γ -producing CD4+ and CD8+ T cells, illustrating the prolonged
180 activation of several T cell subsets beyond the acute infection.



182 **Figure 2: *Toxoplasma gondii* infection induces long-term increase of colonic Th1 CD4+ T cells and cytotoxic**
183 **CD8+ T cells**

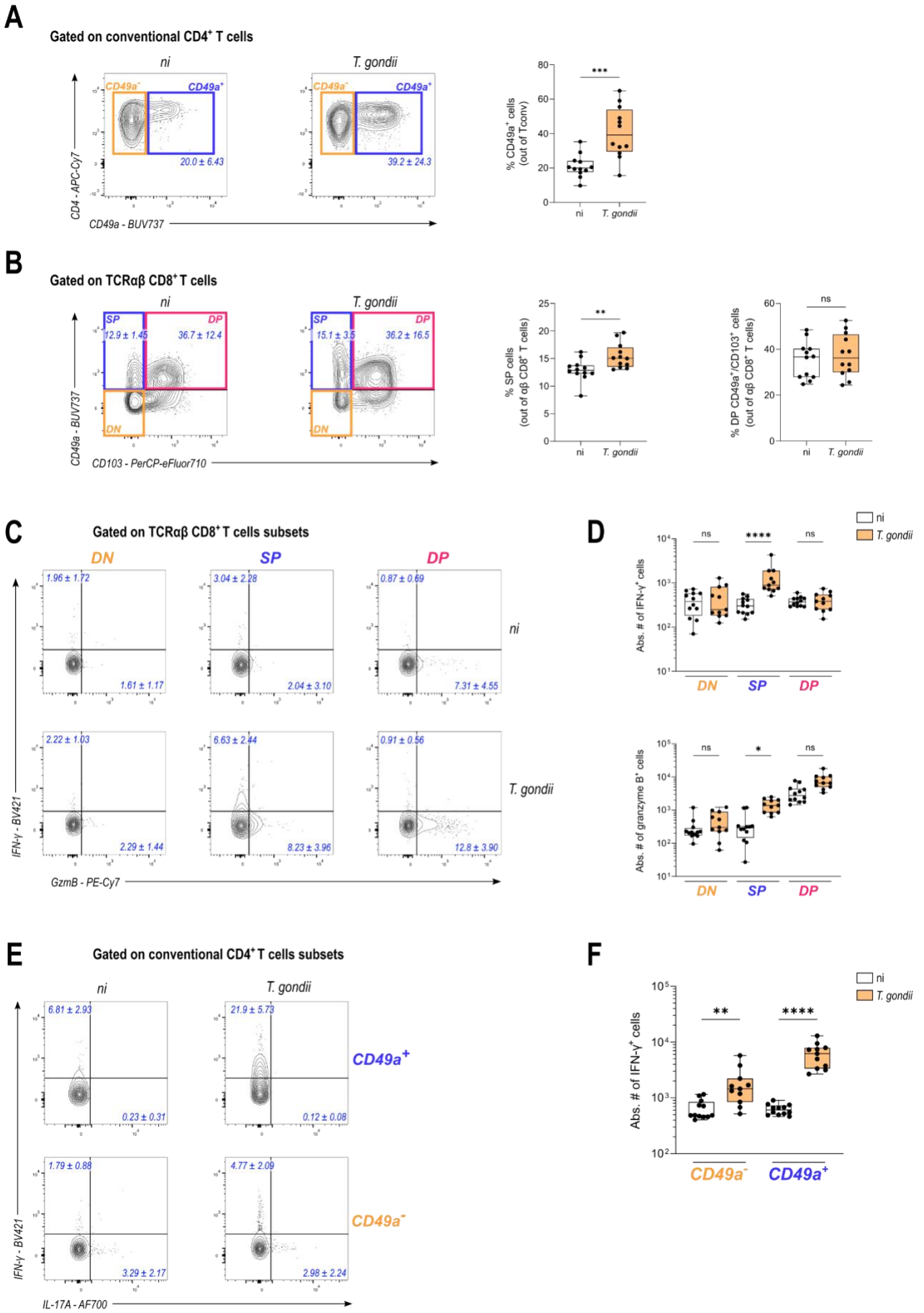
184 **(A-D)** Flow cytometry analysis of the indicated cell subsets in the colon of non-infected (ni) vs. mice chronically ip-infected for 70 days
185 (*T. gondii*). Box and whisker show median +/- IQR. Data are pooled from 2 independent experiments and each dot represents one
186 mouse with a total of 12 (ni) and 11 (*T. gondii*) mice. Statistical analysis was performed using Mann-Whitney test or unpaired Student's
187 t test depending on the normality of the values. **(A)** Box and whisker plots show absolute number of CD45⁺ cells and percentage of
188 immune cell subsets out of total CD45⁺ cells in the colon of mice infected (orange) or not (white) for 70 days. **(B-D)** Representative FACS
189 plot for each condition with numbers (in blue) indicating the median percentage +/- IQR of positive cells among **(B)** conventional (Foxp3-
190) CD4+ T cells, **(C)** TCR $\alpha\beta$ CD8+ T cells and **(D)** TCR $\gamma\delta$ CD8+ T cells. Box and whisker plots show the absolute number (median +/- IQR) of
191 each T cell subset in the colon of non-infected (white) vs infected (orange) mice.

192

193 ***Toxoplasma gondii* infection induces an accumulation of colon-resident memory T cells (Trm)**

194 The above data indicate that chronic *T. gondii* infection is associated with a long-lasting increase of colonic T
195 cells with enhanced effector functions. Since the parasite is cleared from the colon in most mice during chronic
196 phase (see **Fig. 1C**), these data cannot be explained by continuous stimulation of T cells with parasite-derived
197 antigenic peptides in the colon. Instead, this increase could result from the generation and persistence of
198 resident memory T cells in the colon throughout chronic phase. In the brain, it is now well established that *T.*
199 *gondii* infection promotes the generation of parasite-specific brain-resident CD8+ T cells, which sequentially
200 acquire expression of residency markers such as CD69, CD49a and CD103, allowing their retention in the tissue
201 ^{31,36}. To investigate whether T cells persisting in the colon of *T. gondii* chronically infected mice also exhibit a
202 tissue-resident memory phenotype, we examined the expression of CD49a by CD4+ T cells and of CD49a and
203 CD103 by CD8+ T cells. CD103 was not considered for CD4+ T cells since it is more a Treg marker than a
204 meaningful marker of resident CD4+ Tconv, and CD69 could not be used since it is induced by the *in vitro*
205 PMA/ionomycin stimulation step. We found that chronic infection by *T. gondii* leads to an increase in the
206 frequency of CD49a-positive cells among both conventional (Foxp3-) CD4+ and TCR $\alpha\beta$ + CD8+ T cells. However,
207 no difference was found in the frequency of CD49a/CD103 double-positive cells among TCR $\alpha\beta$ + CD8+ T cells
208 (**Fig. 3A-B**). Since we reported above that *T. gondii* chronic infection causes an elevated production of IFN- γ
209 and granzyme B by T cells in the colon, we wondered whether this increased cytokine production could be
210 linked to the increase in colon-resident T cells, as Trm are typically known as fast responders following
211 stimulation. We noticed that infection significantly increased the abundance of resident (CD49a single positive)
212 TCR $\alpha\beta$ + CD8+ T cells able to produce IFN- γ or granzyme B in response to PMA/ionomycin restimulation, while
213 no statistical difference was observed on CD49a-negative or CD49a/CD103 double-positive cells (**Fig. 3C-D**).
214 Similarly, *T. gondii* latent infection caused an increase in conventional CD4+ T cells producing IFN- γ upon
215 PMA/ionomycin restimulation, with the most prominent increase observed among the resident CD49a-positive
216 subset (**Fig. 3E-F**). Combined, these data indicate that chronic infection by *T. gondii* generates CD49a+ Trm that
217 persist in the colon and display heightened effector functions.

218 Since inflammation is often associated with pain, this increase in 'pro-inflammatory' type 1-polarized resident
219 T cells could appear antagonistic with the observed decreased visceral nociceptive responses of chronically
220 infected mice. Importantly, studies have highlighted that effector T cells, in particular CD4+ T cells, can release
221 endogenous opioid peptides called enkephalins, that are able to alleviate pain in different inflammatory
222 contexts, including colitis. Furthermore, it was reported that enkephalins could be produced by colitogenic T
223 cells, highlighting the dual effect of T cells on inflammation and pain modulation ^{37,38}. Based on this, we
224 hypothesized that the release of enkephalins by T cells present in the colon of chronically infected mice may be
225 responsible for the decrease in visceral nociceptive responses.



226

227

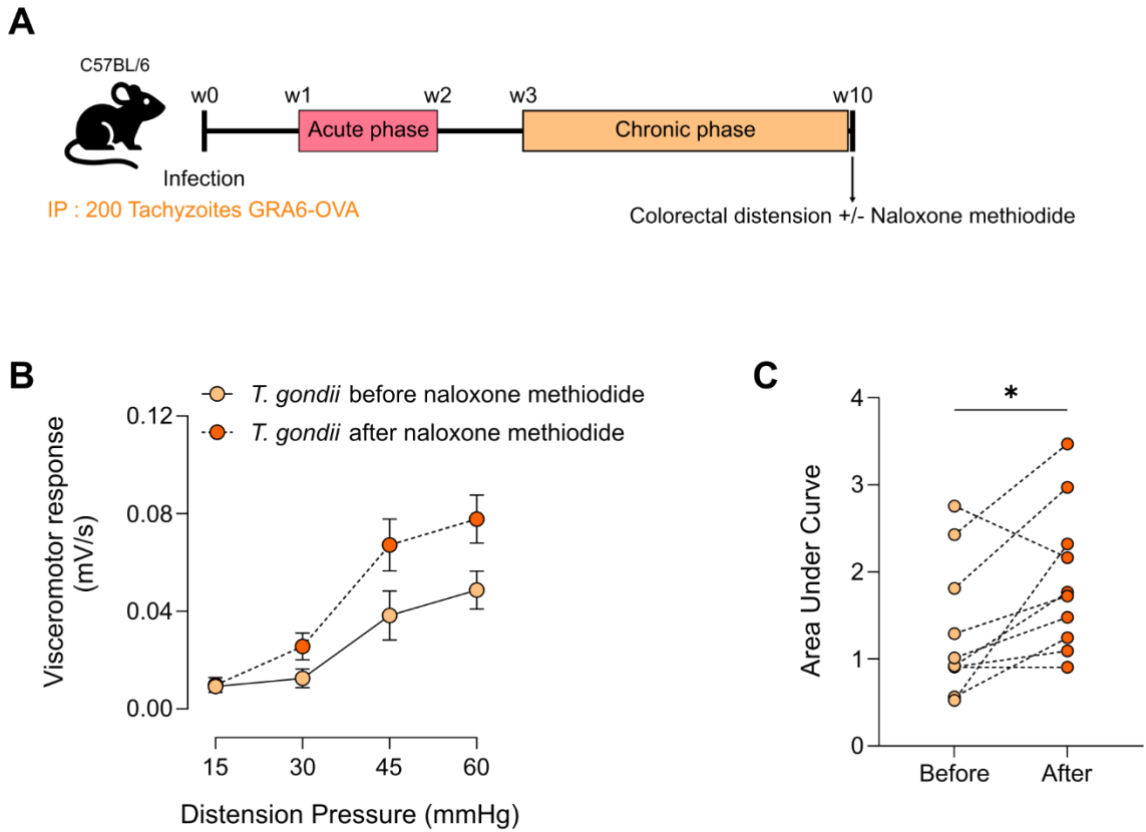
Figure 3: *Toxoplasma gondii* infection generates Th1 CD4⁺ and cytotoxic CD8⁺ resident T cells

228 **(A-F)** FACS plots or Box and whisker plots with median +/- IQR showing absolute number or percentage of cell subsets in the colon of
229 non-infected (ni) or chronically ip-infected mice (*T. gondii*) for 70 days. Data are pooled from 2 independent experiments and each dot
230 represents one mouse with n = 12 (ni) vs. 11 (*T. gondii*). Depending on the normality of the dataset, statistical analysis was performed
231 using Mann-Whitney test or unpaired t test when comparing 2 conditions (A and B), or using Kruskal-Wallis test with Dunn's correction
232 for multiple comparisons (D and F). **(A and B)** Representative FACS plots for each condition with numbers in blue showing median
233 percentage +/- IQR of CD49a-positive cells among **(A)** conventional (Foxp3-) CD4+ T cells and **(B)** TCRαβ+ CD8+ T cells. Corresponding
234 frequency of each T cell subset are represented with box and whisker plots showing median +/- IQR. **(C and D)** Representative FACS plot
235 for each condition with numbers in blue indicating the median percentage +/- IQR of cytokine-positive cells out of TCRαβ CD8+ T cells
236 **(C)** and the absolute number of each subset **(D)**, represented as box and whisker plots showing median +/- IQR. **(E and F)** Representative
237 FACS plots for each condition with numbers in blue indicating the median percentage +/- IQR of cytokine-positive cells out of
238 conventional (Foxp3-) CD4+ T cells **(E)** and the absolute number of each subset **(F)**, represented as box and whisker plots showing median
239 +/- IQR.

240

241 ***Toxoplasma gondii* chronic infection decreases visceral nociceptive responses through peripheral opioid-** 242 **signaling**

243 To assess the contribution of enkephalins produced by T cells in the hypoalgesic phenotype caused by latent *T.*
244 *gondii* infection, we took advantage of a new mouse model enabling constitutive T cell-specific deletion of the
245 pro-enkephalin-encoding gene (Penk). To this aim, we crossed Penk-flox mice³⁹ with CD4-Cre mice. Since most
246 T cells are derived from a thymic precursor stage that co-expressed CD4 and CD8, this CD4-Cre model should
247 allow the deletion of Penk in both mature CD4+ and CD8+ T cells **(Fig. S3A)**. We confirmed by FlowFISH that
248 compared to CD4-Cre- mice, CD4-Cre+ mice display a 10-fold decrease in the percentage of T cells expressing
249 Penk mRNA **(Fig. S3B)**. Using this model in which T cells are able (Penk T^{WT}) or not (Penk T^{KO}) to produce
250 enkephalins, we assessed visceral nociceptive responses to colorectal distension in chronically infected mice
251 **(Fig. S3C)**. Preventing enkephalin production by T cells did not change the visceromotor response of chronically
252 infected mice, suggesting that T cell-released enkephalin peptides are not involved in the regulation of visceral
253 nociception in the context of chronic infection by *T. gondii* **(Fig. S3D)**. Notably, this result suggests the potential
254 contribution of other cellular sources of enkephalins, or even other types of opioids, in the hypoalgesic
255 phenotype. To formally assess the implication of opioid signaling, we tested whether the hypoalgesic
256 phenotype could be reversed by blocking opioid receptors. To restrict the inhibition to peripheral opioid
257 receptor, we used naloxone methiodide, an opioid receptor antagonist which cannot cross the blood brain
258 barrier⁴⁰. We assessed visceral nociception in chronically infected mice before and after naloxone methiodide
259 injection **(Fig. 4A)**. As shown in **Fig. 4B-C**, the administration of naloxone methiodide to infected mice
260 significantly increased nociceptive responses, indicating that peripheral opioid receptor signaling is involved in
261 the hypoalgesic phenotype induced by *T. gondii* chronic infection. The same naloxone methiodide treatment
262 did not change the visceral nociception of uninfected mice **(Fig. S4)**. Therefore, collectively, our data show that
263 peripheral opioid receptor signaling underlies the decreased visceral nociceptive responses observed upon
264 chronic infection by *T. gondii* but that enkephalins produced by T cells do not play a major role in this phenotype.



266

267 **Figure 4: Decreased visceral nociceptive responses induced by *Toxoplasma gondii* chronic infection relies on**
 268 **peripheral opioid signaling**

269 **(A)** Experimental workflow: C57BL/6 were infected with Pru.GFP.GRA6-OVA *T. gondii* by intraperitoneal injection with 200 tachyzoites.
 270 At 10 weeks post-infection, colorectal distension was performed to assess visceral nociception of each mice before or 30 min after
 271 intraperitoneal injection of naloxone-methiodide. **(B)** Visceromotor response (VMR) to increasing colorectal distension pressure (15 to
 272 60 mmHg) was measured in infected mice before (in orange) or after (in red) naloxone methiodide injection. Data are shown as mean
 273 +/- SEM and are from 1 experiment representative of 2 independent experiments with n = 10 mice per experiment. **(C)** Area Under the
 274 Curve (AUC) are represented for each mouse with 2 dots corresponding to the AUC before (in orange) and after (in red) naloxone
 275 methiodide treatment. Statistical analysis was performed using a paired t test.

276 **Discussion**

277 *T. gondii* is a widespread parasite that establishes chronic infection in all warm-blooded animals including
278 humans. While *T. gondii* infection is known to have major consequences on brain functions, the long-term
279 impact of this infection on the gut compartment remains ill-defined. Using a mouse model of latent *T. gondii*
280 infection, this study reports that latent infection downregulates basal visceral nociceptive response measured
281 to colorectal distension. This phenotype was observed both after natural infection (*per os*) and following
282 intraperitoneal administration of tachyzoites, suggesting that the systemic dissemination phase of the parasite,
283 rather than the initial intestinal invasion step, is important for the establishment of the hypoalgesic phenotype.
284 Importantly, we observed that this decreased visceral nociceptive response is dependent on peripheral opioid
285 receptor signaling. Whether the parasite is directly responsible for the desensitization of nociceptive fibers was
286 not formally addressed in our work. However, we think it is unlikely since the hypoalgesic phenotype was
287 observed in a context where *T. gondii* has been cleared from peripheral tissues and the only reservoir of *T.*
288 *gondii* is the CNS. By analogy with the current view that neuroinflammatory pathways more than *T. gondii* cysts
289 themselves, underlie the *T. gondii*-mediated cognitive alterations^{25,41,42}, we suspect that the consequences of
290 chronic *T. gondii* infection on colon pain perception result from local neuroimmune imprinting, leading to a
291 durable shift of the balance towards antinociceptive signals, rather than from a direct manipulation of infected
292 neurons by *T. gondii* in the colon or DRG.

293 In our view, this hypoalgesic phenotype was unexpected for at least two reasons. First, *T. gondii* infection has
294 so far been reported to be an aggravating factor rather than a negative modulator of intestinal inflammation
295 and immunopathology, two conditions that are classically associated with pain. Along this line, one study in
296 humans has revealed a higher seroprevalence of *T. gondii* in Crohn's disease patients, although not in Ulcerative
297 Colitis patients⁴³. In experimental models, analyses of orally infected C57BL/6 mice showed massive
298 inflammatory lesions of the ileum during acute phase^{44,45}, suggesting that *T. gondii* could actually be an
299 infectious trigger of inflammatory bowel disease (IBD)^{46,47}. Accordingly, chronic *T. gondii* encephalitis was
300 recently found to exacerbate the susceptibility of mice to DSS-induced colitis, an established model of IBD²⁷.
301 Data from our paper actually support this hypothesis since we observed that latent *T. gondii* infection mobilizes
302 pro-inflammatory T cells in the colon, including resident T cells, which are known to contribute to chronic
303 intestinal inflammation⁴⁸.

304 Yet, IBD and IBS are notably distinct pathologies. While IBD is characterized by severe and chronic inflammation
305 of the GI tract, IBS is mostly a functional syndrome that is associated with low-grade inflammation or immune
306 activation of the gut, and is generally devoid of overt chronic inflammation. Nevertheless, several
307 gastrointestinal infections have been reported to cause PI-IBS^{16,49}, which is the second reason why our data are
308 unexpected. To our knowledge, only one case-control study explored the association between *T. gondii*
309 exposure and visceral sensitivity⁵⁰. In this study, the seroprevalence of *T. gondii* infection was higher in subjects
310 with frequent abdominal pain (8%) than in control subjects (4%), suggesting an association between *T. gondii*

311 infection and frequent abdominal pain. However, the context of abdominal pain (e.g. IBS, pharmacological
312 treatment and/or infection) was not described, thereby hampering interpretation of this work. Moreover, since
313 it is unknown whether seroconversion preceded or not the onset of abdominal pain, our understanding of the
314 underlying mechanisms remains limited. A serodiagnosis of *T. gondii* exposure in well-characterized cohorts of
315 IBS patients, with a detailed description of clinical symptoms and visceral sensitivity, would be needed to
316 establish to which extent our data translate to the human setting.

317 An important mechanistic achievement of our study is to show that opioid receptor signaling in peripheral
318 neurons underlies *T. gondii*-induced hypoalgesia of the colon but that T cell-produced enkephalins play only a
319 limited or redundant role in this phenotype. These observations raise the question of the nature of the
320 endogenous opioid(s) involved and its cellular source(s). Visceral nociception results from the integration of
321 both pro- and anti-nociceptive signals in the gut, which potentially involve different cell types and opioids, and
322 which could also be modulated by changes in expression of the opioid receptors themselves and/or activity of
323 their signaling pathways. Hence, the hypoalgesic phenotype could involve multiple mechanisms acting on one
324 or several of these processes. As various cell types are able to produce different opioids^{33,35,51}, an increased
325 opioid receptor activity could arise from a heightened opioid secretion not only by T cells, but also by
326 macrophages, Tuft cells and/or neurons, possibly explaining the lack of effect of a single Penk deletion in T cells.
327 We initially focused on enkephalins since Penk transcripts were the only detectable mRNA for endogenous
328 opioids in the colon tissue (i.e. Pdyn transcripts coding for dynorphin and Pomc transcripts coding for
329 proopiomelanocortin/ β -endorphin were undetectable). Quantifying changes in bioactive opioid peptides in
330 the colon microenvironment upon chronic *T. gondii* infection would be useful but the absence of reliable tools
331 to perform this at the single-cell level represents a major roadblock preventing us from tackling this question.
332 Alternatively, it is possible that other (non-opioid) molecules may be involved, provided that such molecules
333 may be capable of modulating the opioid receptor signaling pathway. Of note, serotonin (5-hydroxytryptamine,
334 5-HT) is a pro-nociceptive mediator able to directly activate neurons⁵². In the GI tract, 5-HT is mainly produced
335 by enterochromaffin cells (EC cells), a subset of enteroendocrine cells located within the epithelium.
336 Importantly, EC cells transduce luminal signals to mucosal nerve endings, producing various effects including
337 nociceptor sensitization leading to visceral hypersensitivity⁵³. Moreover, several studies have reported
338 alteration of serotonin metabolism in IBS patients^{54,55}, suggesting that serotonin signaling could alter pain
339 perception in the gut. In line with these observations, a recent study highlighted a link between serotonin and
340 opioid signaling since both pathways act on PKA activity, though in an opposite manner. More precisely, a
341 decreased serotonin signaling was associated with an enhanced opioid receptor signaling, resulting in a
342 prolonged endogenous analgesia⁵⁶. Serotonin release by EC cells can be triggered by various stimuli, including
343 short chain fatty acids produced by the gut microbiota or neurotransmitters⁵², which may be dysregulated upon
344 *T. gondii* chronic infection. Elucidating the potential implication of the serotonergic pathway in *T. gondii*-
345 induced hypoalgesia could be an interesting avenue for future investigation.

346 Based on the abundance of the microbiota in the colon and the pleiotropic effects exerted by gut microbiota
347 on the host including the production of 5-HT⁵⁷ and the modulation of opioid receptor-mediated analgesia⁵⁸,
348 another attractive hypothesis is that changes in visceral nociception caused by chronic *T. gondii* infection may
349 arise from long-lasting alteration of gut commensals. To date, experimental studies have shown that acute *T.*
350 *gondii* infection causes a clear dysbiosis in the colon, characterized in particular by an increase in
351 *Enterobacteriaceae*^{59,60}. However, the extent of colon dysbiosis during chronic infection appears more variable,
352 with studies reporting either no impact on gut microbiota^{27,59} and studies showing mild modifications in the
353 *Bacteroidetes* and *Firmicute* phyla^{61,62}. While *T. gondii* chronic infection does not induce dramatic changes in
354 the microbiota, we cannot rule out the possibility that subtle alterations in the abundance of some specific
355 species might suffice to modulate visceral nociceptive responses in our mouse model. Notably, a study has
356 highlighted the capacity of a particular bacterial species, *L. reuteri*, to upregulate opioid receptor expression,
357 thereby preventing visceral hypersensitivity in a rat model of colon obstruction⁵⁸.

358 In conclusion, our work not only provides the first detailed mapping of immune changes that persist in the colon
359 throughout latent infection, but it also uncovers a new and unexpected consequence of *T. gondii* chronic
360 infection on host intestinal homeostasis. We report that *T. gondii* latent infection elicits a prolonged
361 modification of the colonic T cell compartment as well as a decreased visceral nociceptive response to colorectal
362 distension. This hypoalgesia depends on peripheral opioid receptor signaling but is independent from
363 enkephalins produced by T cells, suggesting that other cell types and/or other opioids may be involved. These
364 data support the notion that *T. gondii* is likely not a driver of post-infectious IBS, and they even suggest that
365 latent *T. gondii* infection could be negatively associated with abdominal pain in humans.

366

367 **Materials & Methods**

368 **Mice**

369 C57BL/6 (B6) and CBA/J mice were purchased from Janvier (France). PenkT^{KO} mice were obtained by crossing
370 Penkfl/fl mice with CD4-Cre mice (B6.Cg-Tg(Cd4-cre)1Cwi/BfluJ from JAX, ref 022071). All non-commercial
371 mouse models were housed and bred under specific pathogen-free conditions at the 'Centre Regional
372 d'Exploration Fonctionnelle et de Ressources Experimentales' (CREFRE-Inserm UMS006). Mice were housed
373 under a 12h light/dark cycle and were experimentally infected between 8 and 10 weeks of age. All mice used
374 in experiments were males. Number of mice and experimental replicates are indicated in the respective figure
375 legends. Animal care and used protocols were carried out under the control of the French National Veterinary
376 Services and in accordance with the current European regulations (including EU Council Directive, 2010/63/EU,
377 September 2010). The protocols APAFIS 20921-2019052311562282 and APAFIS 14513-2018040313435341v6
378 were approved by the local Ethical Committee for Animal Experimentation registered by the "Comité National
379 de Réflexion Ethique sur l'Experimentation Animale" under no. CEEA122.

380

381 ***Toxoplasma gondii* culture and experimental infections**

382 Human Foreskin Fibroblasts (HFF) were cultured in Dulbecco's Modified Eagle Medium (DMEM, Gibco)
383 supplemented with Glutamax, sodium pyruvate, 10% vol/vol FBS (Gibco), 1% vol/vol Penicillin/Streptomycin
384 (Gibco) and 0.1% vol/vol 2-β-mercaptoethanol (Gibco). Pru-GFP.GRA6-OVA tachyzoites were grown *in vitro* on
385 confluent HFF in DMEM supplemented with 1% vol/vol FBS (Gibco). *In vitro* cultured parasites were filtered
386 through a 3 μm polycarbonate hydrophilic filter (it4ip S.A.) and diluted in sterile PBS before infection of mice
387 with 200 tachyzoites. For cyst generation, CBA/J mice were infected by intraperitoneal injection with 200
388 tachyzoites. After 2 months, brains of infected CBA mice were collected and homogenized before performing
389 a rhodamine-conjugated Dolichos Biflorus Agglutinin (Vector Laboratories) labelling. Cysts were counted using
390 an inverted fluorescence microscope. After cyst enumeration, brain homogenate was diluted in sterile PBS to
391 orally infect mice by gavage with 10 cysts.

392

393 **Parasite load quantification (DNA extraction, qPCR)**

394 Genomic DNA (gDNA) was extracted from tissue homogenate using the DNeasy Blood & Tissue Kit (Qiagen). All
395 tissues analyzed were snap frozen in liquid nitrogen directly after isolation before storage at -80°C. For brain
396 and colon, tissues were kept frozen in liquid nitrogen and crushed to obtain a fine powder used to isolate gDNA
397 according to manufacturer's recommendations. gDNA was quantified using a Nanodrop and the number of
398 parasite per μg of tissue DNA was calculated by qPCR using the TOX9/TOX11 primers and a standard curve made

399 of a known number of corresponding parasites (as described in ⁶³). The quantification threshold indicates the
400 highest dilution of the standard curve, above which parasite concentration could be extrapolated.

401

402 **Hematoxylin/Eosin (H/E) stainings**

403 Colonic tissues were fixed for 24h in 4% formaldehyde and then transferred in 70% ethanol at 4°C. Tissues were
404 embedded in paraffin to perform tissue sections (5 µm thickness) and Hematoxylin/Eosin stainings.

405

406 **Isolation of colonic cells & PMA/ionomycin restimulation**

407 After mouse euthanasia, the colon was collected, opened longitudinally and kept on ice in RPMI supplemented
408 with 10% FBS. Tissue was cut into small pieces before incubation in RPMI supplemented with 5% FBS and
409 500mM EDTA to remove epithelial cells and intraepithelial lymphocytes (IEL) for 30 min at 4°C under agitation.
410 Supernatant (containing IEL) was filtered through 40 µm cell strainer, washed once and kept on ice until Percoll
411 gradient. The remaining tissue was then digested in RPMI supplemented with 10% FBS, 1 M HEPES, 220 U/mL
412 Collagenase VIII (Sigma) and 10 µg/mL DNase I (Sigma) for 1 hour at 37°C under agitation. The supernatant was
413 collected, filtered through a 70 µm cell strainer, washed and pooled with the IEL fraction, and kept on ice. The
414 remaining tissue was digested a second time with the same digestion buffer for 50 min at 37°C under agitation.
415 At the end, tissue was mechanically dissociated with a 18G needle attached to a 5 mL syringe. Cells were filtered
416 through a 70 µm cell strainer before being pooled with the other fractions. Cells were then isolated using a
417 30% Percoll gradient diluted in RPMI at 4°C. Cell suspension was used directly for flow cytometry staining, or
418 restimulated for 3.5 h at 37°C 5% CO₂ in complete RPMI supplemented 0.05 µg/mL Phorbol 12-myristate 13-
419 acetate (PMA), 1 µg/mL ionomycin and 3 µg/mL Brefeldin A (BfA). Cells were then washed with FACS buffer
420 (2% FBS and 2mM EDTA) before performing flow cytometry stainings.

421

422 **Flow cytometry stainings & analysis**

423 For flow cytometry, after Fc receptor saturation and dead cell detection with fixable viability dye, cells were
424 surface stained for 30 min at 4°C. Cells were then washed and fixed using the Foxp3/transcription factor
425 staining buffer set (Invitrogen) before performing intracellular staining to detect cytokines and transcription
426 factors according to the manufacturer's recommendations. Flow cytometry analyses were performed using
427 FlowJo and OMIQ (unsupervised analyses) softwares.

428

429 **Antibodies used in this study**

Antibody	Clone	Fluorochrome	Dilution	Reference	Provider
Anti-mouse CD16/62	93	N/A	50	101302	Biologend
Fixable Viability Dye	N/A	eFluor780	1000	65-0865-14	eBioscience
CD3ε	145-2C11	BV711	50	100349	Biologend
CD3ε	145-2C11	APC	100	100312	Biologend
CD4	GK1.5	APC-Cy7	200	552051	BD Pharmingen
CD8α	53-6.7	BV786	300	563332	BD Horizon
CD11b	M1/70	PE-CF594	2000	562287	BD Horizon
CD11c	HL3	PerCP-Cy5.5	100	560584	BD Pharmingen
CD19	6D5	APC	100	115512	Biologend
CD45	30-f11	PE	1000	103105	Biologend
CD45.2	104	AF488	300	109815	Biologend
CD49a	Ha31/8	BUV737	300	741776	BD OptiBuild
CD90.2	53-2.1	PE-Cy7	500	25-0902-82	eBioscience
CD103	2E7	PerCP-eFluor710	200	46-1031-82	eBioscience
CD117 (c-kit)	2B8	BV785	200	105841	Biologend
EpCAM	G8.8	APC	500	118213	Biologend
EpCAM	G8.8	PE-dazzle594	800	118235	Biologend
F4/80	BM8	AF700	100	123130	Biologend
FCεRI	MAR-1	APC-Cy7	200	134325	Biologend
Foxp3	NRRF-30	PE	200	12-4771-82	eBioscience
Gata3	TWAJ	AF488	100	53-9966-42	eBioscience
Granzyme B	QA16A02	PE-Cy7	200	372214	Biologend
IFNγ	XMG1.2	BV421	200	563376	BD Horizon
IL17	TC11-18H10	AF700	200	560820	BD Pharmingen
Ly6C	HK1.4	BV711	2000	128037	Biologend
Ly6G	1A8	BV510	200	127633	Biologend
NK1.1	PK136	BV650	100	564143	BD Horizon
RORγt	Q31-378	BV421	200	562894	BD Horizon
TCRγδ	GL3	BV510	200	118131	Biologend
CD8a	53-6.7	BV421	200	563898	BD Horizon
CD44	IM7	BV605	200	563058	BD Horizon
CD4	RM4-5	PE-CF594	800	562285	BD Horizon
CD62L	MEL-14	PE-Cy7	300	560516	BD Pharmingen
Penk probes	N/A	AF647	20	PF-204	Invitrogen

430

431 Table 1. List of antibodies and conditions used in flow cytometry experiments.

432 **FlowFISH stainings**

433 Spleen from Penk^{fllox/fllox} / CD4^{Cre} mice was smashed on a 100 μm cell strainer (Falcon) before performing red
434 blood cell lysis. Splenocytes were then stained with the PrimeFlow RNA Assay Kit (Invitrogen) and the anti-
435 mouse Penk probe set (Invitrogen #PF-204) according to the manufacturer's protocol. Briefly, cells were first
436 labelled with antibodies as described above with the reagent provided in the kit. A second fixation step was
437 performed after the intracellular staining before proceeding to the FISH staining. For FISH staining, cells were
438 incubated with the anti-mouse Penk probe set (1:20) for 2h at 40°C. After washes, cells were kept overnight at
439 4°C in wash buffer containing RNase inhibitors. The day after, amplification steps were performed to increase
440 the signal: cells were first incubated with pre-amplification mix during 1.5 h at 40°C, washed and then incubated
441 with amplification mix for an additional 1.5 h at 40°C. Cells were then incubated with the label probes (Alexa
442 Fluor 647, 1:100) for 1h at 40°C.

443

444 **Colorectal distension and visceromotor response measurements**

445 Visceral nociception was assessed by measuring the visceromotor response (VMR) to increasing colorectal
446 distension pressures (15, 30, 45, 60 mm Hg) with at least 5 min rest between each distension pressure. Three
447 days before distension, mice were anaesthetized with ketamine (10 mg/kg) and xylazine (1 mg/kg) to implant
448 2 electrodes (Bioflex insulated wire AS631; Cooner Wire, Chatsworth, CA) into abdominal external oblique
449 muscles. Electrodes were exteriorized at the back of the neck and protected by a plastic tube attached to the
450 skin. After surgery, mice were monitored during the next 3 days for abnormal behavior. The day of the
451 distension, electrodes were connected to a Bio Amp, itself connected to an electromyogram acquisition system
452 (ADInstruments, Inc., Colorado Springs, CO). Ten (10) second-long distensions were performed on conscious
453 animals with a 10.5 mm diameter balloon catheter (Fogarty catheter for arterial embolectomy) gently inserted
454 into the distal colon at 5 mm from the anus (balloon covering a distance of 1cm). Electromyography activity of
455 abdominal muscles was recorded to calculate visceromotor responses using LabChart 8 software
456 (ADInstruments).

457

458 **Statistical analysis**

459 Statistical analysis was performed using GraphPad Prism 10.1 software. For all panels, normality was assessed
460 with D'Agostino & Pearson tests. When normal, a parametric test was applied as indicated in the figure legend.
461 If not, a non-parametric analysis was performed. * or #: $p < 0.05$, **: $p < 0.01$, ***: $p < 0.001$, ****: $p < 0.0001$.
462 Modalities of data representation and statistical tests are indicated in the respective figure legends.

463

464

465 **ACKNOWLEDGEMENTS**

466 We thank N. Vergnolle for critical reading of the manuscript, R. Balouzat, R. Ecalard, F. Chaboud, E. Debon, M.A.
467 El Manfaloti, S. Negroni, J. Leblond, S. Fresse, M. Lulka from ANEXPLO-CREFRE UMS006 for ethical care of our
468 models, F. L’Faqihi-Olive, V. Duplan-Eche, A.-L. Iscache, H. Garnier from the flow cytometry core facilities of
469 Infinity for expert technical assistance, R. Miranda-Capet, E. Valdevit and A. Herrmann for technical help. We
470 thank S. Milia and F. Abella from the the Experimental Histopathology Facility of Inserm / UPS / ENVY US006
471 CREFRE-Anexplor, Toulouse Purpan for technical assistance.

472 This work was supported by institutional grants from Inserm, PIA PARAFRAP Consortium (ANR-11-LABX0024 to
473 NB), “Agence Nationale pour la Recherche” (ANR-19-CE15-0008 TRANSMIT to FM/NB; ANR-22-CE14-0053
474 NINTENDO to NB ; ANR-22-CE15-0018 ImmunUP to NB), “Fondation pour la Recherche sur le Cerveau” AAP2021
475 to NB. AA was supported by a doctoral fellowship from the French Minister of Research and a 4th year PhD
476 fellowship from “Fondation pour la Recherche Médicale” (FRM FDT202304016672).

477

478

479 **CONTRIBUTIONS**

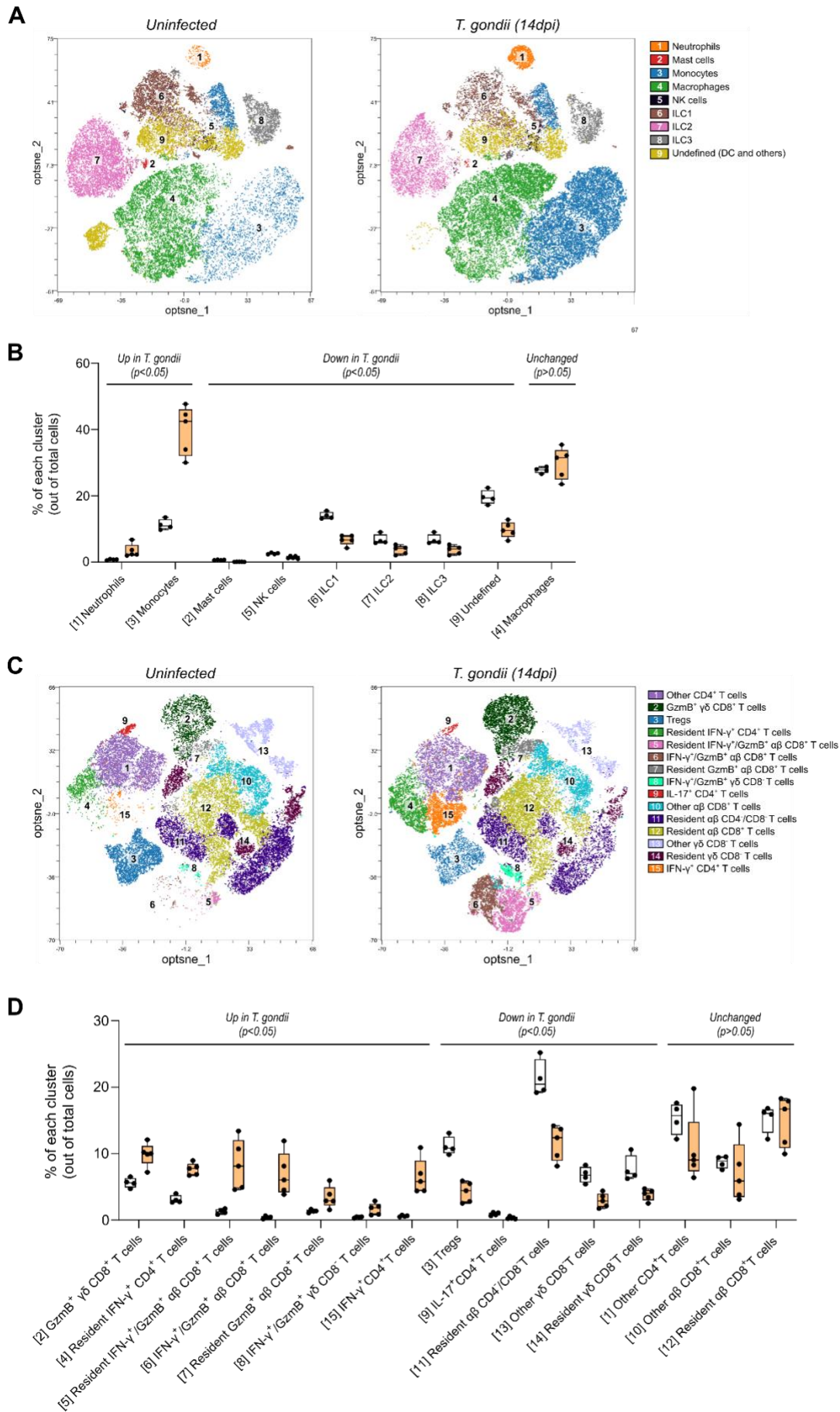
480 AA, FM, NC, GD, CB, NB designed experiments. AA, XMO, LR, MB, EB, NC, CB performed experiments. AA, XMO,
481 LR, MB, EB, FM, NC, GD, CB, NB analyzed experiments. GM contributed mice and expert advice on the Penkfl/fl
482 mouse model. FM provided the CD4-Cre model and expert consulting. AA, NB & CB wrote the manuscript. All
483 co-authors read, edited, and approved the final manuscript.

484

485 **ETHICAL DECLARATIONS**

486 The authors declare no competing interests.

487



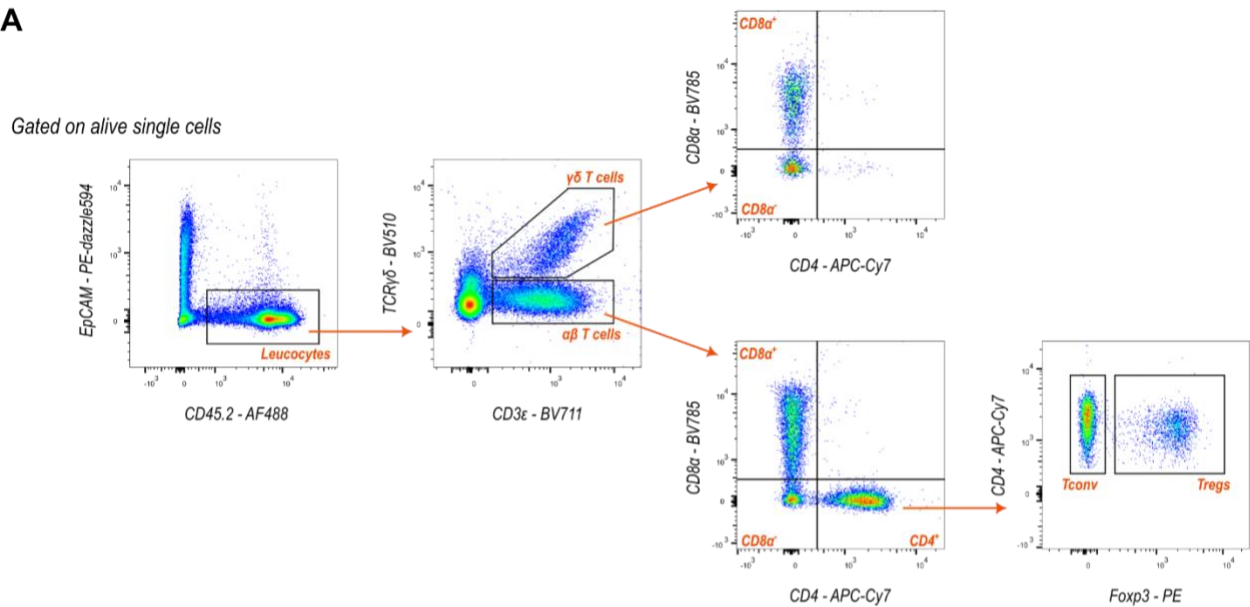
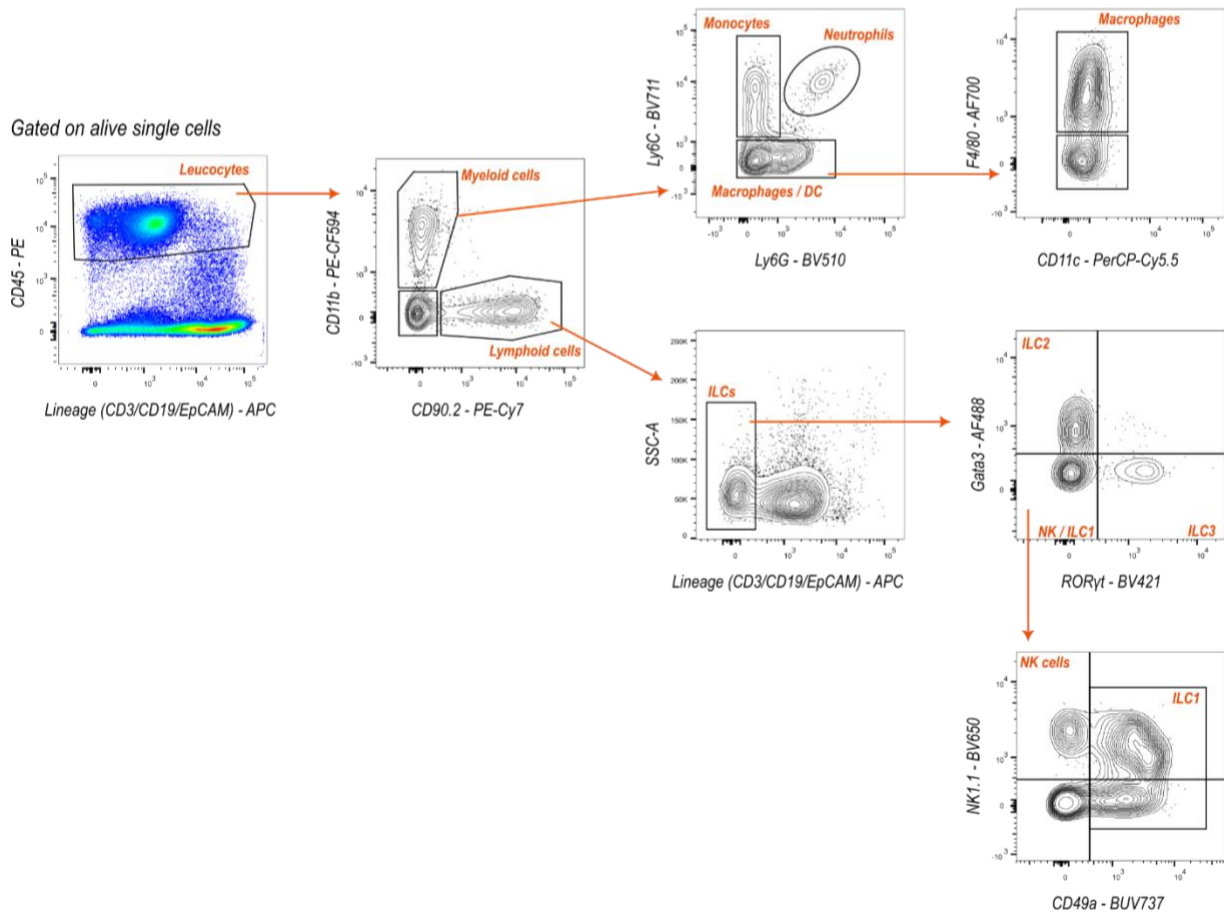
488

489 **Figure S1: Acute *T. gondii* infection induces recruitment of myeloid cells and T cells in the colon**

490 **(A and B)** Unsupervised analysis with flow cytometry data obtained from the colon of non-infected or ip-infected mice at acute stage
491 (14 days post-infection) was performed using OMIQ software. Statistical analysis was performed using a Mann-Whitney test on each
492 subpopulation and summarized into one single graph. **(A)** Unsupervised analysis was performed on live CD45⁺ cells negative for CD3ε,
493 CD19 and EpCAM (called Lin-negative cells). Opt-SNE plot of 34 000 Lin-negative cells concatenated from 4 non-infected mice (left) and
494 42 500 Lin-negative cells concatenated from 5 infected mice (right), divided in 9 clusters using Phenograph algorithm, based on the
495 expression of surface markers associated with each cell subset. Table under opt-sne shows the relative abundance of each cluster in
496 each condition (infected (orange) or not (white)). **(B)** Unsupervised analysis was performed on live T cells using the following gating
497 strategy: EpCAM⁻ / CD45⁺ / CD3⁺. Opt-SNE plot of 36 360 colonic T cells concatenated from 4 non-infected mice (left) and 45 450 colonic
498 T cells concatenated from 5 infected mice (right), divided in 15 clusters using Phenograph algorithm, based on the expression of different
499 markers. Table under opt-sne shows the relative abundance of each cluster in each condition (infected (orange) or not (white)).

500

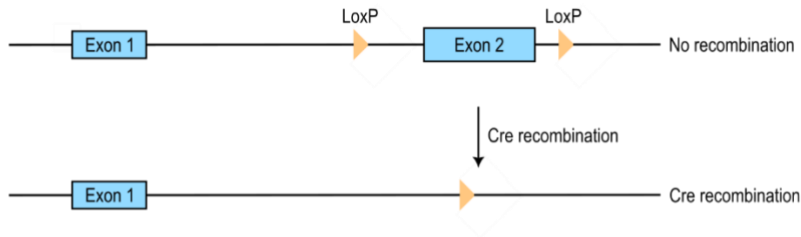
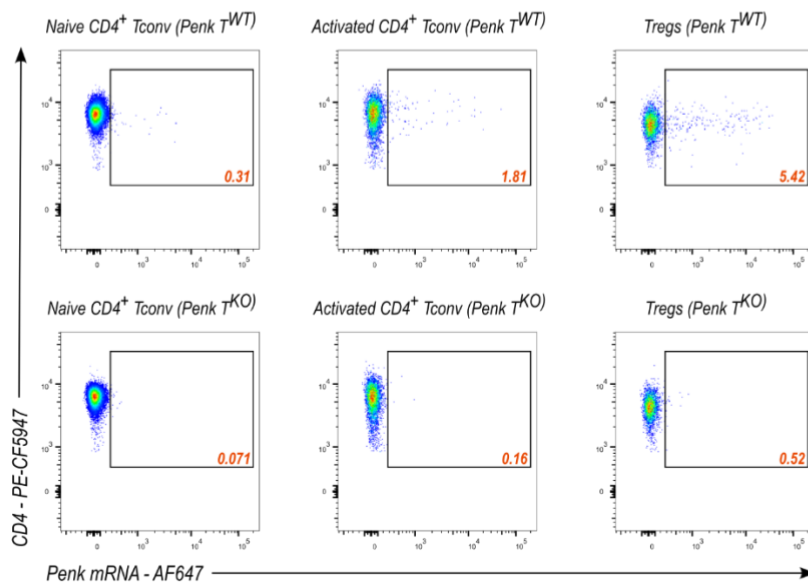
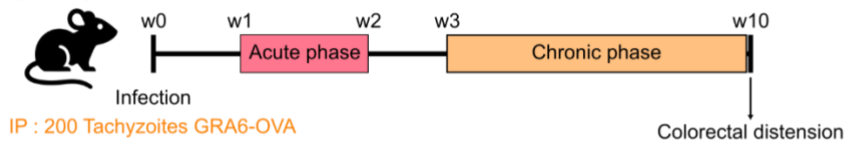
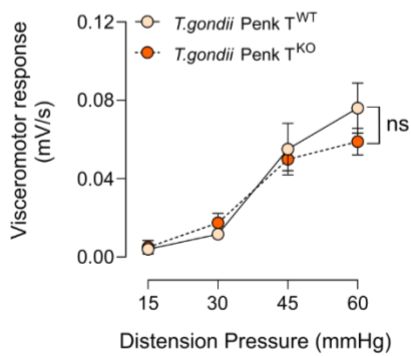
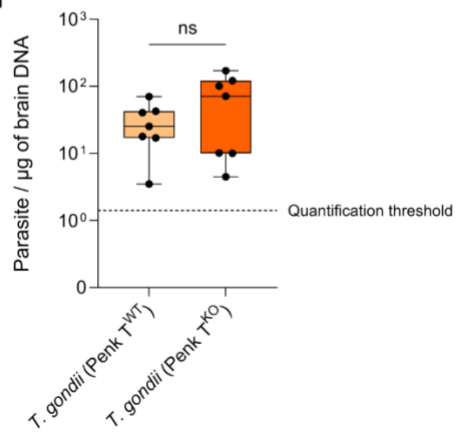
501

A**B**

502

503 **Figure S2 (related to Figure 2): Gating strategies used to identify the immune populations in the colon**

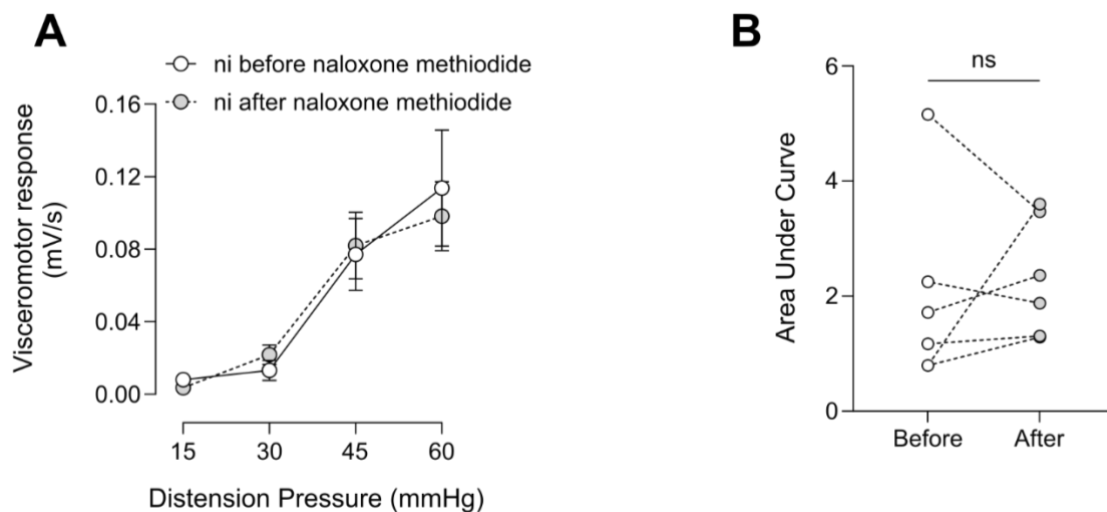
504 (A and B) Cell doublets were excluded using double gating on SSC-A vs. SSC-H followed by SSC-W vs. SSC-H exclusion. Dead cells were
 505 removed using a viability marker to allow analysis of live cells only. Arrows indicate the order of the gating strategy. (A) Gating strategy
 506 used to identify the different T cell subsets in the colon. (B) Gating strategy used to identify the different cell subsets belonging to the
 507 myeloid and Innate Lymphoid Cells (ILC) lineages.

APenk^{flox} / CD4^{Cre}**B****C**Penk^{flox} / CD4^{Cre}**D****F**

509 **Figure S3 (related to Figure 4): *T. gondii*-induced decrease in nociceptive responses is independent of T-cell**
510 **derived enkephalins**

511 **(A)** Mouse model for T cell-specific deletion of enkephalin-encoding gene (Penk) in mice. Penk-floxed mice carrying LoxP sites upstream
512 and downstream of Penk exon 2 were crossed with transgenic mice expressing the Cre recombinase under the CD4 promoter (CD4-Cre).
513 **(B)** Genomic DNA was extracted from CD4+ T cells sorted from the spleen of CD4-Cre positive (Penk T^{KO}) or negative (Penk T^{WT}) mice.
514 Deletion of Penk exon 2 was assessed by qPCR using 2 sets of primers to amplify the exons 1 and 2. The set of primer used in each
515 condition is indicated in blue and primers location is represented in panel A. **(C)** Deletion of Penk was confirmed by measuring the
516 expression of Penk mRNA by flow cytometry (FlowFISH) in naïve (CD62L+/CD44-) or activated (CD44+) conventional (FoxP3-) CD4+ T
517 cells, and in regulatory CD4+ T cells (Foxp3+). **(D)** Experimental workflow: C57BL/6 expressing (Penk T^{WT}) or not (Penk T^{KO}) in T cells
518 were infected with the Pru.GFP.GRA6-OVA *T. gondii* by intraperitoneal injection with 200 tachyzoites. At 10 weeks post-infection,
519 colorectal distension was performed to assess visceral sensitivity. **(E)** Visceromotor response (VMR) to increasing colorectal distension
520 pressure (15 to 60 mm Hg) was measured in chronically ip-infected mice invalidated (Penk T^{KO}) or not (Penk T^{WT}) for Penk gene in T cells.
521 VMR are represented with mean +/- SEM with n = 7 Penk T^{WT} vs 6 Penk T^{KO} animals. Statistical analysis was performed on Areas Under
522 the Curve (AUC) with a Mann-Whitney test using GraphPad Prism. Data correspond to one experiment. **(F)** Parasite loads in the brain
523 were measured by qPCR on genomic DNA for each mouse, showing no difference between Penk T^{WT} and Penk T^{KO} infected mice.

524



525

526 **Figure S4 (related to Figure 4) : Naloxone methiodide treatment has no impact on visceral nociceptive**
527 **responses at steady state**

528 **(A and B)** Colorectal distension was performed to assess visceral sensitivity of each mice before (in white) or 30 min after (in gray)
529 intraperitoneal injection of naloxone-methiodide. **(A)** Visceromotor response (VMR) in response to increasing colorectal distension
530 pressure (15 to 60mmHg) was measured in uninfected mice (ni) treated or not with Naloxone methiodide. Data are shown as mean +/-
531 SEM and are from 1 experiment representative with n = 6 mice. **(B)** Area Under the Curve (AUC) are represented for each mouse with 2
532 dots corresponding to the AUC before (in white) and after (in gray) naloxone methiodide treatment. Statistical analysis was performed
533 using a Wilcoxon's test.

- 536 1 Hassan, A. & Blanchard, N. Microbial (co)infections: Powerful immune influencers. *PLoS pathogens* **18**,
537 e1010212, doi:10.1371/journal.ppat.1010212 (2022).
- 538 2 Bach, J. F. The hygiene hypothesis in autoimmunity: the role of pathogens and commensals. *Nat Rev*
539 *Immunol* **18**, 105-120, doi:10.1038/nri.2017.111 (2018).
- 540 3 Maizels, R. M. & McSorley, H. J. Regulation of the host immune system by helminth parasites. *J Allergy*
541 *Clin Immunol* **138**, 666-675, doi:10.1016/j.jaci.2016.07.007 (2016).
- 542 4 Steinbach, K. *et al.* Brain-resident memory T cells generated early in life predispose to autoimmune
543 disease in mice. *Sci Transl Med* **11**, doi:10.1126/scitranslmed.aav5519 (2019).
- 544 5 Bjornevik, K. *et al.* Longitudinal analysis reveals high prevalence of Epstein-Barr virus associated with
545 multiple sclerosis. *Science* **375**, 296-301, doi:10.1126/science.abj8222 (2022).
- 546 6 Sardinha-Silva, A., Alves-Ferreira, E. V. C. & Grigg, M. E. Intestinal immune responses to commensal and
547 pathogenic protozoa. *Front Immunol* **13**, 963723, doi:10.3389/fimmu.2022.963723 (2022).
- 548 7 Vergnolle, N. Protease inhibition as new therapeutic strategy for GI diseases. *Gut* **65**, 1215-1224,
549 doi:10.1136/gutjnl-2015-309147 (2016).
- 550 8 Verma-Gandhu, M. *et al.* CD4+ T-cell modulation of visceral nociception in mice. *Gastroenterology* **130**,
551 1721-1728, doi:10.1053/j.gastro.2006.01.045 (2006).
- 552 9 Boue, J., Blanpied, C., Brousset, P., Vergnolle, N. & Dietrich, G. Endogenous opioid-mediated analgesia
553 is dependent on adaptive T cell response in mice. *J Immunol* **186**, 5078-5084,
554 doi:10.4049/jimmunol.1003335 (2011).
- 555 10 Kavelaars, A. & Heijnen, C. J. Immune regulation of pain: Friend and foe. *Sci Transl Med* **13**, eabj7152,
556 doi:10.1126/scitranslmed.abj7152 (2021).
- 557 11 Lee, Y. Y., Annamalai, C. & Rao, S. S. C. Post-Infectious Irritable Bowel Syndrome. *Current*
558 *gastroenterology reports* **19**, 56, doi:10.1007/s11894-017-0595-4 (2017).
- 559 12 Enck, P. *et al.* Irritable bowel syndrome. *Nature reviews. Disease primers* **2**, 16014,
560 doi:10.1038/nrdp.2016.14 (2016).
- 561 13 Halliez, M. C. *et al.* *Giardia duodenalis* induces paracellular bacterial translocation and causes
562 postinfectious visceral hypersensitivity. *Am J Physiol Gastrointest Liver Physiol* **310**, G574-585,
563 doi:10.1152/ajpgi.00144.2015 (2016).
- 564 14 Alsaady, I. M. *Cryptosporidium* and irritable bowel syndrome. *Tropical parasitology* **14**, 8-15,
565 doi:10.4103/tp.tp_10_23 (2024).
- 566 15 Porter, C. K. *et al.* Postinfectious gastrointestinal disorders following norovirus outbreaks. *Clin Infect Dis*
567 **55**, 915-922, doi:10.1093/cid/cis576 (2012).
- 568 16 Downs, I. A., Aroniadis, O. C., Kelly, L. & Brandt, L. J. Postinfection Irritable Bowel Syndrome: The Links
569 Between Gastroenteritis, Inflammation, the Microbiome, and Functional Disease. *Journal of clinical*
570 *gastroenterology* **51**, 869-877, doi:10.1097/MCG.0000000000000924 (2017).
- 571 17 Balemans, D. *et al.* Evidence for long-term sensitization of the bowel in patients with post-infectious-
572 IBS. *Sci Rep* **7**, 13606, doi:10.1038/s41598-017-12618-7 (2017).
- 573 18 Defaye, M. *et al.* Fecal dysbiosis associated with colonic hypersensitivity and behavioral alterations in
574 chronically *Blastocystis*-infected rats. *Sci Rep* **10**, 9146, doi:10.1038/s41598-020-66156-w (2020).
- 575 19 Ibeakanma, C. *et al.* *Citrobacter rodentium* colitis evokes post-infectious hyperexcitability of mouse
576 nociceptive colonic dorsal root ganglion neurons. *The Journal of physiology* **587**, 3505-3521,
577 doi:10.1113/jphysiol.2009.169110 (2009).
- 578 20 Pappas, G., Roussos, N. & Falagas, M. E. Toxoplasmosis snapshots: global status of *Toxoplasma gondii*
579 seroprevalence and implications for pregnancy and congenital toxoplasmosis. *International journal for*
580 *parasitology* **39**, 1385-1394, doi:10.1016/j.ijpara.2009.04.003 (2009).
- 581 21 Snyder, L. M. & Denkers, E. Y. From Initiators to Effectors: Roadmap Through the Intestine During
582 Encounter of *Toxoplasma gondii* With the Mucosal Immune System. *Frontiers in cellular and infection*
583 *microbiology* **10**, 614701, doi:10.3389/fcimb.2020.614701 (2020).
- 584 22 Hand, T. W. *et al.* Acute gastrointestinal infection induces long-lived microbiota-specific T cell
585 responses. *Science* **337**, 1553-1556, doi:10.1126/science.1220961 (2012).

- 586 23 Weiss, L. M. & Kim, K. The development and biology of bradyzoites of *Toxoplasma gondii*. *Front Biosci*
587 **5**, D391-405, doi:10.2741/weiss (2000).
- 588 24 Cerutti, A., Blanchard, N. & Besteiro, S. The Bradyzoite: A Key Developmental Stage for the Persistence
589 and Pathogenesis of Toxoplasmosis. *Pathogens* **9**, doi:10.3390/pathogens9030234 (2020).
- 590 25 Laing, C., Blanchard, N. & McConkey, G. A. Noradrenergic Signaling and Neuroinflammation Crosstalk
591 Regulate *Toxoplasma gondii*-Induced Behavioral Changes. *Trends in immunology* **41**, 1072-1082,
592 doi:10.1016/j.it.2020.10.001 (2020).
- 593 26 Vyas, A. Mechanisms of Host Behavioral Change in *Toxoplasma gondii* Rodent Association. *PLoS*
594 *pathogens* **11**, e1004935, doi:10.1371/journal.ppat.1004935 (2015).
- 595 27 Saraav, I. *et al.* Chronic *Toxoplasma gondii* infection enhances susceptibility to colitis. *Proc Natl Acad*
596 *Sci U S A* **118**, doi:10.1073/pnas.2106730118 (2021).
- 597 28 Gois, M. B. *et al.* Chronic infection with *Toxoplasma gondii* induces death of submucosal enteric neurons
598 and damage in the colonic mucosa of rats. *Exp Parasitol* **164**, 56-63, doi:10.1016/j.exppara.2016.02.009
599 (2016).
- 600 29 Machado, C. C. A. *et al.* *Toxoplasma gondii* infection impairs the colonic motility of rats due to loss of
601 myenteric neurons. *Neurogastroenterology and motility : the official journal of the European*
602 *Gastrointestinal Motility Society* **33**, e13967, doi:10.1111/nmo.13967 (2021).
- 603 30 Salvioni, A. *et al.* Robust Control of a Brain-Persisting Parasite through MHC I Presentation by Infected
604 Neurons. *Cell reports* **27**, 3254-3268 e3258, doi:10.1016/j.celrep.2019.05.051 (2019).
- 605 31 Porte, R. *et al.* Protective function and differentiation cues of brain-resident CD8+ T cells during
606 surveillance of latent *Toxoplasma gondii* infection. *Proc Natl Acad Sci U S A* **121**, e2403054121,
607 doi:10.1073/pnas.2403054121 (2024).
- 608 32 Gonzalez-Rodriguez, S. *et al.* Hyperalgesic and hypoalgesic mechanisms evoked by the acute
609 administration of CCL5 in mice. *Brain Behav Immun* **62**, 151-161, doi:10.1016/j.bbi.2017.01.014 (2017).
- 610 33 Basso, L. *et al.* Mobilization of CD4+ T lymphocytes in inflamed mucosa reduces pain in colitis mice:
611 toward a vaccinal strategy to alleviate inflammatory visceral pain. *Pain* **159**, 331-341,
612 doi:10.1097/j.pain.0000000000001103 (2018).
- 613 34 Basso, L. *et al.* T-lymphocyte-derived enkephalins reduce Th1/Th17 colitis and associated pain in mice.
614 *Journal of gastroenterology* **53**, 215-226, doi:10.1007/s00535-017-1341-2 (2018).
- 615 35 Labuz, D., Celik, M. O., Seitz, V. & Machelska, H. Interleukin-4 Induces the Release of Opioid Peptides
616 from M1 Macrophages in Pathological Pain. *The Journal of neuroscience : the official journal of the*
617 *Society for Neuroscience* **41**, 2870-2882, doi:10.1523/JNEUROSCI.3040-20.2021 (2021).
- 618 36 Landrith, T. A. *et al.* CD103+ CD8 T Cells in the *Toxoplasma*-Infected Brain Exhibit a Tissue-Resident
619 Memory Transcriptional Profile. *Front Immunol* **8**, 335, doi:10.3389/fimmu.2017.00335 (2017).
- 620 37 Boue, J. *et al.* Endogenous regulation of visceral pain via production of opioids by colitogenic CD4(+) T
621 cells in mice. *Gastroenterology* **146**, 166-175, doi:10.1053/j.gastro.2013.09.020 (2014).
- 622 38 Basso, L. *et al.* Endogenous analgesia mediated by CD4(+) T lymphocytes is dependent on enkephalins
623 in mice. *J Neuroinflammation* **13**, 132, doi:10.1186/s12974-016-0591-x (2016).
- 624 39 Aubert, N. *et al.* Enkephalin-mediated modulation of basal somatic sensitivity by regulatory T cells in
625 mice. *eLife* **13**, doi:10.7554/eLife.91359 (2024).
- 626 40 Lewanowitsch, T. & Irvine, R. J. Naloxone methiodide reverses opioid-induced respiratory depression
627 and analgesia without withdrawal. *European journal of pharmacology* **445**, 61-67, doi:10.1016/s0014-
628 2999(02)01715-6 (2002).
- 629 41 Martynowicz, J., Augusto, L., Wek, R. C., Boehm, S. L., 2nd & Sullivan, W. J., Jr. Guanabenz Reverses a
630 Key Behavioral Change Caused by Latent Toxoplasmosis in Mice by Reducing Neuroinflammation. *MBio*
631 **10**, doi:10.1128/mBio.00381-19 (2019).
- 632 42 Belloy, M. *et al.* Chronic IL-1-induced DNA double-strand break response in hippocampal neurons drives
633 cognitive deficits. *BioRxiv 2024* <https://biorxiv.org/cgi/content/short/2024.02.03.578747v1> (2024).
- 634 43 Lidar, M. *et al.* Infectious serologies and autoantibodies in inflammatory bowel disease: insinuations at
635 a true pathogenic role. *Ann N Y Acad Sci* **1173**, 640-648, doi:10.1111/j.1749-6632.2009.04673.x (2009).
- 636 44 Buzoni-Gatel, D. *et al.* Murine ileitis after intracellular parasite infection is controlled by TGF-beta-
637 producing intraepithelial lymphocytes. *Gastroenterology* **120**, 914-924 (2001).
- 638 45 Bonnart, C. *et al.* Protease-activated receptor 2 contributes to *Toxoplasma gondii*-mediated gut
639 inflammation. *Parasite Immunol* **39**, doi:10.1111/pim.12489 (2017).

- 640 46 Liesenfeld, O. Oral infection of C57BL/6 mice with *Toxoplasma gondii*: a new model of inflammatory
641 bowel disease? *The Journal of infectious diseases* **185 Suppl 1**, S96-101, doi:10.1086/338006 (2002).
- 642 47 Egan, C. E., Cohen, S. B. & Denkers, E. Y. Insights into inflammatory bowel disease using *Toxoplasma*
643 *gondii* as an infectious trigger. *Immunology and cell biology* **90**, 668-675, doi:10.1038/icb.2011.93
644 (2012).
- 645 48 Zundler, S. *et al.* Hobit- and Blimp-1-driven CD4(+) tissue-resident memory T cells control chronic
646 intestinal inflammation. *Nat Immunol* **20**, 288-300, doi:10.1038/s41590-018-0298-5 (2019).
- 647 49 Dai, C. & Jiang, M. The incidence and risk factors of post-infectious irritable bowel syndrome: a meta-
648 analysis. *Hepato-gastroenterology* **59**, 67-72, doi:10.5754/hge10796 (2012).
- 649 50 Alvarado-Esquivel, C. *et al.* Association between *Toxoplasma gondii* exposure and abdominal pain: An
650 age- and gender-matched case-control seroprevalence study. *European journal of microbiology &*
651 *immunology*, doi:10.1556/1886.2024.00025 (2024).
- 652 51 Gerbe, F. *et al.* Distinct ATOH1 and Neurog3 requirements define tuft cells as a new secretory cell type
653 in the intestinal epithelium. *J Cell Biol* **192**, 767-780, doi:10.1083/jcb.201010127 (2011).
- 654 52 Bellono, N. W. *et al.* Enterochromaffin Cells Are Gut Chemosensors that Couple to Sensory Neural
655 Pathways. *Cell* **170**, 185-198 e116, doi:10.1016/j.cell.2017.05.034 (2017).
- 656 53 Bayrer, J. R. *et al.* Gut enterochromaffin cells drive visceral pain and anxiety. *Nature* **616**, 137-142,
657 doi:10.1038/s41586-023-05829-8 (2023).
- 658 54 Vahora, I. S., Tsouklidis, N., Kumar, R., Soni, R. & Khan, S. How Serotonin Level Fluctuation Affects the
659 Effectiveness of Treatment in Irritable Bowel Syndrome. *Cureus* **12**, e9871, doi:10.7759/cureus.9871
660 (2020).
- 661 55 Keszthelyi, D. *et al.* Visceral hypersensitivity in irritable bowel syndrome: evidence for involvement of
662 serotonin metabolism--a preliminary study. *Neurogastroenterology and motility : the official journal of*
663 *the European Gastrointestinal Motility Society* **27**, 1127-1137, doi:10.1111/nmo.12600 (2015).
- 664 56 Isensee, J. *et al.* Synergistic regulation of serotonin and opioid signaling contributes to pain insensitivity
665 in Nav1.7 knockout mice. *Science signaling* **10**, doi:10.1126/scisignal.aah4874 (2017).
- 666 57 Sanidad, K. Z. *et al.* Gut bacteria-derived serotonin promotes immune tolerance in early life. *Science*
667 *immunology* **9**, eadj4775, doi:10.1126/sciimmunol.adj4775 (2024).
- 668 58 Hegde, S., Lin, Y. M., Fu, Y., Savidge, T. & Shi, X. Z. Precision *Lactobacillus reuteri* therapy attenuates
669 luminal distension-associated visceral hypersensitivity by inducing peripheral opioid receptors in the
670 colon. *Pain* **161**, 2737-2749, doi:10.1097/j.pain.0000000000001967 (2020).
- 671 59 Raetz, M. *et al.* Parasite-induced TH1 cells and intestinal dysbiosis cooperate in IFN-gamma-dependent
672 elimination of Paneth cells. *Nat Immunol* **14**, 136-142, doi:10.1038/ni.2508 (2013).
- 673 60 Heimesaat, M. M. *et al.* Gram-negative bacteria aggravate murine small intestinal Th1-type
674 immunopathology following oral infection with *Toxoplasma gondii*. *J Immunol* **177**, 8785-8795,
675 doi:10.4049/jimmunol.177.12.8785 (2006).
- 676 61 French, T. *et al.* Persisting Microbiota and Neuronal Imbalance Following *T. gondii* Infection Reliant on
677 the Infection Route. *Front Immunol* **13**, 920658, doi:10.3389/fimmu.2022.920658 (2022).
- 678 62 Hatter, J. A. *et al.* *Toxoplasma gondii* infection triggers chronic cachexia and sustained commensal
679 dysbiosis in mice. *PLoS ONE* **13**, e0204895, doi:10.1371/journal.pone.0204895 (2018).
- 680 63 Feliu, V. *et al.* Location of the CD8 T Cell Epitope within the Antigenic Precursor Determines
681 Immunogenicity and Protection against the *Toxoplasma gondii* Parasite. *PLoS pathogens* **9**, e1003449,
682 doi:10.1371/journal.ppat.1003449 (2013).

683

684